

DNA Binding Is Not Sufficient for H-NS-mediated Repression of *proU* Expression*

(Received for publication, January 22, 1997)

Bart J. A. M. Jordi‡, Anne E. Fielder, Christopher M. Burns, Jay C.D. Hinton, Nir Dover§, David W. Ussery, and Christopher F. Higgins¶

From the Nuffield Department of Clinical Biochemistry, and Imperial Cancer Research Fund Laboratories, Institute of Molecular Medicine, University of Oxford, John Radcliffe Hospital, Oxford OX3 9DU, United Kingdom

H-NS is a major component of bacterial chromatin and influences the expression of many genes. H-NS has been shown to exhibit a binding preference for certain AT-rich curved DNA elements *in vitro*. In this study we have addressed the factors that determine the specificity of H-NS action *in vitro* and *in vivo*. In bandshift studies, H-NS showed a slight binding preference for all curved sequences tested whether GC-based or AT-based; the specific architecture of the curve also influenced H-NS binding. In filter retention assays little difference in affinity could be detected for any sequence tested, including the downstream regulatory element (DRE) a downstream curved DNA element required for H-NS to repress transcription of the *Salmonella typhimurium proU* operon *in vivo*. A K_d of 1–2 μM was estimated for binding of H-NS to each of these sequences. *In vivo*, the distance between the *proU* promoter and the DRE, their relative orientations on the face of the DNA helix, and translation of the DRE had no major effect on *proU* regulation. None of the synthetic curved sequences tested could functionally replace the DRE *in vivo*. These data show that differential binding to curved DNA cannot account for the specificity of H-NS action *in vivo*. Furthermore, binding of H-NS to DNA *per se* is insufficient to repress the *proU* promoter. Thus, the DRE does not simply act as an H-NS binding site but must have a more specific role in mediating H-NS regulation of *proU* transcription.

H-NS is a 15.6-kDa polypeptide, one of the two most abundant proteins associated with the bacterial nucleoid. H-NS has a role in chromosome organization (1, 2). Consistent with this role, H-NS compacts DNA (3, 4) and can constrain DNA supercoils *in vitro* (5). Plasmids isolated from *hns* mutants have altered levels of supercoiling (6–8), and plasmid and chromosomal DNA supercoiling is altered in *hns* mutants *in vivo* (9). In addition to its role in chromosome organization, H-NS influences the expression of several independently regulated genes, many of which are modulated in response to changing environmental conditions (2). The precise mechanism by which H-NS modulates transcription is unknown.

* This work was supported in part by the Wellcome Trust and Imperial Cancer Research Fund. The costs of publication of this article were defrayed in part by the payment of page charges. This article must therefore be hereby marked "advertisement" in accordance with 18 U.S.C. Section 1734 solely to indicate this fact.

‡ Supported by a European Union Fellowship.

§ EMBO short term Fellow. Present address: Division of Microbial and Molecular Ecology, Institute of Life Sciences, The Hebrew University of Jerusalem, Jerusalem 91904, Israel.

¶ Howard Hughes International Research Scholar. To whom correspondence should be addressed. Tel.: 44-1865-222423; Fax: 44-1865-222431.

The binding of H-NS to DNA is relatively nonspecific (3, 5, 10). This raises a paradox. How does H-NS influence transcription at only a subset of promoters? Part of the explanation may come from the observation that H-NS exhibits a binding preference for certain intrinsically curved DNA sequences *in vitro* (11–14) and that, at least at some promoters, curved DNA elements are required for H-NS action *in vivo* (13). Indeed, it may be that curved DNA sequence elements are required for the action of H-NS at all promoters (15–17). However, for the limited number of DNA curves studied, the increased preference for curved DNA, compared with nonspecific binding to generic DNA, is only a few-fold (5, 12, 13, 18). Furthermore, as curved DNA sequences are found near most promoters, including many promoters that are not responsive to H-NS (for review see Ref. 19), it is not clear how specificity is achieved. Finally, the distance between the curve and the RNA polymerase binding site can be varied up to 200 bp.¹ Thus, it is unclear whether DNA curvature *per se* is the principal factor that determines H-NS action or how the interaction of H-NS and curved sequences might influence promoter function.

To address the mechanisms by which H-NS affects transcription we have used the *proU* promoter of *Salmonella typhimurium* as a model. *proU* encodes a transport system for the osmoprotectant glycine betaine, and its expression is increased when cells are exposed to high extracellular osmolarity (20–23). *proU* appears to be one of the simplest H-NS-responsive promoters as no *trans*-acting factor, other than H-NS itself, appears to be required for its regulation. *proU* expression is derepressed in *hns* mutants (6, 7, 24), although residual osmoregulation is retained (13, 25, 26). Repression of *proU* by H-NS requires an intrinsically curved region of DNA located around 200 bp downstream of the transcription start site, within the first structural gene of the *proU* operon (the downstream regulatory element, DRE) (12, 26–28). However, the binding preference of H-NS for the DRE *in vitro* is, at most, only a few-fold greater than for generic DNA, and the precise distance between the DRE and the *proU* promoter does not appear to be critical (13, 25, 26). It is not known how interaction of H-NS with the DRE might influence transcription.

In this paper, we have addressed the factors that determine the specificity of H-NS action both *in vivo* and *in vitro*. Consistent with previous reports, a binding preference for curved DNA was detected under certain conditions, although this preference was found to be limited and cannot account for the specificity of action of H-NS *in vivo*. Furthermore, the binding of H-NS to DNA *per se* is insufficient to account for the effects of H-NS on *proU* expression. Thus, the DRE cannot simply provide a site for H-NS binding but must serve a more specific role in H-NS-mediated gene regulation.

¹ The abbreviations used are: bp, base pair(s); DRE, downstream regulatory element; PCR, polymerase chain reaction.

EXPERIMENTAL PROCEDURES

Bacterial Strains and Plasmids—Wild-type *S. typhimurium* LT2 and its congenic derivatives CH1838 (*hns-1::Kan^r*) and CH1833 (*zde-1710::mTn10*) were used for expression studies (8). Note that *zde-1710::mTn10* has no phenotype but was used solely for strain construction (8). All plasmids were constructed and maintained in *Escherichia coli recA* strains prior to electroporation into the appropriate *S. typhimurium* strain. Cells were grown with aeration at 37 °C in LB (29).

Plasmids Containing Curved and Noncurved DNA Inserts—To generate defined curved and noncurved DNA fragments, complementary oligonucleotides (Table I) were annealed, ligated together, and separated by electrophoresis in a 3% NuSieve agarose gel. Ligated fragments of an appropriate size (100–200 bp) were isolated from the gel using a QIAEX gel extraction kit (Qiagen). The overhanging ends of the fragments were filled in with the Klenow fragment of DNA polymerase and ligated into the *EcoRV* site of pBluescript I SK(–) (Stratagene). Three plasmids were generated in this manner, containing the GC curve (pAF1), GC noncurve (pAF2), and AT planar curve (pAF3). Two closely related plasmids containing the AT curve (pTP4) and AT noncurve (pTP5) have been described previously (13). A sixth plasmid (pAF6) was constructed by ligating a 200-bp fragment encompassing the *S. typhimurium proU* DRE (base pair +99 through +299; Ref. 30) between the *NotI* and *SpeI* sites of pBluescript II SK(–). The 200-bp fragment was generated by PCR using primers +99 (5'GGGCGGCCG-CATATTTGGAGAGCATCCG-3') and +299 (5'GGACTAGTTTCAAT-CAGGCGATTGAGAAGG-3') which incorporate sites for *NotI* and *SpeI* to facilitate cloning. The nature and size of the DNA inserts in these plasmids are given in Table II.

To clone these curved/noncurved sequences between the *proU* promoter and the *lacZ* reporter gene, a multiple cloning site was created in plasmid pAV399 (13). Plasmid pAV399 contains the *proU* promoter region (–217 through +100, where +1 is the start of the transcription) (30), directing transcription of the *lacZ* reporter gene. A 51-bp polylinker was inserted into the *EcoRI* site between the *proU* promoter and *lacZ* gene. The polylinker was constructed by annealing two complementary oligonucleotides, 5'AATTCATACGCGGCCGCAAGTCTAGACTTACTAGTACTGGTACCTATGCG-3' and 5'AATTCGCATAGG-TACCAGTACTAGTCAAGTCTAGACTTGGCGCCGCGTAT-3', containing *NotI*, *SpeI*, *XbaI*, and *KpnI* restriction sites and an *EcoRI* site overhang at each end. The resulting plasmid, pAF450, was used as a vector for the construction of a further six plasmids in which curved or noncurved fragments were inserted into the polylinker. Five of the inserts were the curved and noncurved fragments from pAF1, pAF2, pAF3 (excised with *EcoRI* and *HindIII*), pTP4 and pTP5 (excised with *BamHI* and *EcoRI*). The sixth was a 200-bp fragment, generated by the PCR, encompassing the *S. typhimurium proU* DRE (bp +99 through +299) and incorporating terminal *NotI* and *SpeI* sites.

Plasmids with Altered Distances between the *proU* Promoter and the Downstream Curve—pSJ4 contains the same 317-bp *proU* promoter fragment (bp –217 to +100) as pAV399, cloned into the *EcoRI* site upstream of the luciferase reporter genes in pSB71 (Table II). A *SalI-SacI* fragment from pSJ4, containing the *proU* promoter coupled to the *luxAB* reporter genes, was cloned into the pALTER vector (Promega). Using the Altered Sites[®] *in vitro* mutagenesis system (Promega), unique sites for the restriction endonucleases *NcoI* and *BglII* were introduced at bp +17 and +31, respectively (Fig. 1). The mutated *SalI-SacI* fragment was recloned into pSJ4 generating plasmid pBJ1. Plasmids pBJ2, pBJ4, pBJ5, and pBJ6 were generated from pBJ1 by inserting appropriate DNA fragments between the *NcoI* and *BglII* sites (Fig. 1). Plasmid pBJ2 contains a 210-bp fragment *NcoI-BglII* fragment obtained by PCR amplification of the *trp-lacZ* fusion from plasmid pCH133 (13, 31). Plasmids pBJ4, pBJ5, and pBJ6 were generated by ligating the following oligonucleotides (and their complementary strands) between the *NcoI* and *BglII* sites, increasing the distance between the *proU* promoter and DRE by 5, 10, and 15 bp, respectively: pBJ4, 5'GAATTCATGGCTATATCGCCGATAGATCTGAATTC 3'; for pBJ5, 5'GAATTCATGGCTATATCGCCGATGAAAGAGATCTGAATTC 3'; for pBJ6, 5'GAATTCATGGCTATATCGCCGATGAAAGCG-GCGGATCTGAATTC3'.

Anomalous Migration of DNA Fragments—Curved and noncurved DNA fragments were isolated by restriction enzyme digestion and gel purification. Fragments were electrophoresed on a 12% polyacrylamide gel at 5 °C in TBE buffer (32), visualized by ethidium bromide staining, and relative mobility measured compared with standard markers.

DNA Bandshift Studies—H-NS protein from *S. typhimurium* was purified as described (13) and stored at 1–2 mg/ml at –20 °C in 50%

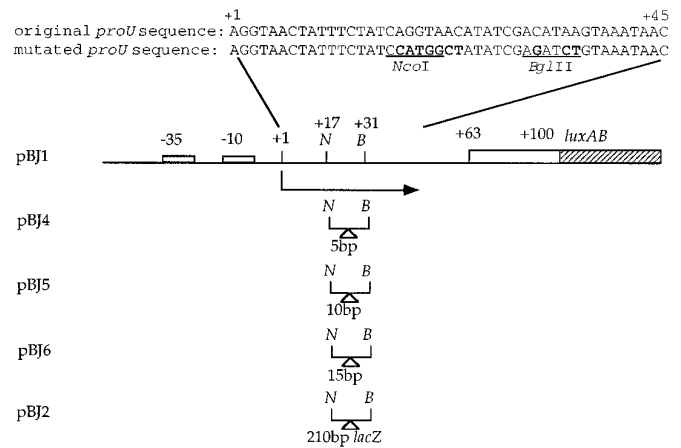


FIG. 1. Schematic of plasmids with inserts between the *proU* promoter and *luxAB* reporter genes. The –35 and –10 regions of the *proU* promoter are indicated. The first 12 amino acids of the *proU* coding sequence from the normal translation initiation site (bp +63 to +100 relative to the start of transcription) are indicated by an open box, and the *luxAB* reporter genes are indicated by a hatched box. The sequences between +1 and +45 of the original and the mutated *proU* genes are given. Mutated nucleotides are shown in bold. The unique restriction sites *NcoI* and *BglII* introduced at position +17 and +31 are indicated. Details of the fragments introduced between these two sites to create pBJ2 and pBJ4–pBJ6 are given under “Experimental Procedures.”

glycerol. 1 μ g of plasmid DNA digested with *HaeIII* was incubated in 9 μ l of binding buffer (10 mM Tris-Cl pH 7.5, 15 mM KCl, 2 mM spermidine, 15% glycerol, 0.1 mM EDTA), together with 1 μ l of H-NS diluted (in binding buffer) to the appropriate concentration, for 2 min at 20 °C. The samples were electrophoresed on a 3% Metaphor agarose gel at room temperature at 4 V/cm. The DNA was visualized by staining with ethidium bromide.

For competition bandshift studies, appropriate curved or noncurved DNA fragments were isolated from plasmids by restriction enzyme digestion and gel purification. A typical bandshift reaction was carried out in a volume of 15 μ l and contained 1 μ g of H-NS protein, 10 ng of radiolabeled DNA, the indicated amount of competitor DNA, in buffer (10 mM $\text{KH}_2\text{PO}_4/\text{K}_2\text{HPO}_4$, pH 7.6, 15 mM KCl, 0.1 mM EDTA). The reaction was incubated at room temperature for 30 min, and 5 μ l of loading buffer (50% glycerol, 2.5% bromophenol blue) was added to the reaction. Samples were loaded onto a 5% polyacrylamide gel in TBE and electrophoresed at 8 V/cm at 5 °C for 2 h. After electrophoresis the gel was dried and radiolabeled DNA detected by autoradiography.

Filter Retention Assays—Radiolabeled DNA fragments, extending from 77 bp upstream to 51 bp downstream of the polylinker, were amplified from plasmids pAF451–456 using Vent DNA polymerase (New England Biolabs) as directed by the manufacturer, but using only 100 μ M each dNTP and with [α -³²P]dCTP included at 2 μ Ci/nmol. The amplified fragments were purified from 5% polyacrylamide gels and quantitated by liquid scintillation spectroscopy. DNA binding reactions (20 μ l) were done in FR buffer (10 mM Tris-Cl, pH 7.5, 15 mM KCl, 10 mM dithiothreitol, 5 mM MgCl_2 , 1 mM spermidine, 0.1 mM EDTA) using 5–10 ng of radiolabeled DNA and amounts of H-NS ranging from 0.17 to 1.67 μ g. Reactions were incubated at room temperature for 10 min and then filtered under vacuum on Biotrace NT filters (Gelman). The filters were washed with 5 volumes of FR buffer minus spermidine, dried, and the radioactivity retained on the filters determined using a Molecular Dynamics PhosphorImager.

DNA Manipulations—Standard methods were used for gel electrophoresis and the construction of recombinant plasmids (32). Plasmid DNA was electroporated into *S. typhimurium* using a Gene Pulser[®] (Bio-Rad) according to the manufacturer's instructions. One pulse was applied, at capacitance 25 microfarads, resistance 200 Ω , and voltage 2.45 kV. Electrocompetent *S. typhimurium* were prepared as described (13).

Reporter Gene Assays—Cells were grown in low osmolarity medium (see below) to an A_{600} between 0.3 and 0.5. The culture was then split and NaCl added to one-half of the culture to a final concentration of 0.3 M to give an osmotic upshock. The other half of the culture provided a low osmolarity control. The cells were grown for a further 40 min and β -galactosidase or luciferase activities assayed as described previously

TABLE I
Sequences of DNA oligonucleotides used in this study to generate curved and noncurved DNA fragments

Name	Motif	Sequence	Ref.
AT curve	A ₅ N ₅	5' GGCAAAAACG 3' 3' GTTTTTGCC 5'	44
AT noncurve	A ₅ N ₁₀	5' CCGGCAAAAACGGGC 3' 3' CCGTTTTTGCCCGG 5'	44
AT planar curve	A ₅ A ₆	5' TCTCTAAAAAATATATAAAAA 3' 3' TTTTTTATATATTTTAGAGA 5'	36
GC curve	CCGG-N ₇ - CCGG-N ₆	5' CTCCGGATAGGCTCCGGATAG 3' 3' CTATCCGAGGCCATCGAGGC 5'	34
GC noncurve	None	5' CGCATGTACCGACGCATGAG 3' 3' CAGTGGCTGCGTACTCGCGTA 5'	34

(13). Note that using transient osmotic shock, rather than growing cells to steady state at different osmolarities, circumvents possible effects of osmolarity on plasmid copy number and on mRNA stability. For luciferase assays, NB (Difco) was used as the low osmolarity medium; for β -galactosidase assays LB with NaCl omitted was used as the low osmolarity medium. All data are the result of multiple independent determinations. For β -galactosidase assays the data are presented after correction for background expression using data obtained from an identical plasmid lacking a promoter upstream of the reporter gene (pAV250).

RESULTS

Construction of Plasmids Containing Synthetic Curved and Noncurved DNA Fragments

Previous studies have shown that H-NS exhibits a binding preference for curved DNA resulting from phased A tracts. To ascertain whether H-NS recognizes DNA curvature *per se* or the A tracts responsible for curvature, a series of plasmids was constructed containing curved and noncurved DNA fragments (Table I). The base composition of each curved and noncurved pair was similar, but the order of the bases resulted in distinct architectures. One pair of fragments was the AT curve and AT noncurve described previously; H-NS binds to the AT curve preferentially (12, 13). A second pair of curved and noncurved fragments (the GC curve and GC noncurve) were constructed which did not contain A tracts. The GC curve contains the motif "CCGG" in phase with the pitch of the DNA helix (an average of once every 10.5 bp) and has been shown previously to be curved by anomalous electrophoretic mobility and ligation assays (33–35). The GC noncurve has a similar base composition to the GC curve but is designed such that the DNA is much less curved. A fifth DNA fragment (AT planar curve) contained an AT-rich curve designed to be planar (36), in contrast to the nonplanar AT curve described above. The sixth fragment was the DRE from downstream of the *S. typhimurium proU* promoter (bp +99 to +299). Five of the synthetic DNA fragments were generated from the appropriate oligonucleotides (Table I), whereas the sixth fragment, the DRE, was amplified by the PCR. All fragments were cloned into pBluescript. These plasmids, and the sizes of the inserted curved and noncurved DNA fragments, are described in Table II.

Characterization of Curved and Noncurved DNA Fragments

Computer Predictions—Fig. 2 shows the predicted structures of 120-bp fragments formed by ligation of the five different oligonucleotides determined by the CURVATURE program (37). *Panel A* shows the predicted helical path of the AT curve. Note that this curve is "out of plane" with the axis of the DNA helix with the end of the fragment pointing into the plane of the page. *Panel B* shows the AT noncurve in which the A tracts are out of phase. This sequence has several small "snake-like" curves although, on average, the helical path is straight. *Panel C* shows the predicted path of the GC curve. The curvature is

not predicted to be as great as for the AT curve, but it is "in plane" (*i.e.* the path of a longer piece of DNA would form a flat mini-circle as opposed to the superhelical path of the curve in *panel A*). *Panel D* depicts the GC noncurve, of similar base composition to the GC curve (Table I). The fragment is slightly curved, although less so than the GC curve, and is probably closest to "generic" DNA of all the fragments depicted. The AT planar curve depicted in *panel E* is in plane, such that a 126-bp fragment will form a flat mini-circle (36). *Panel F* shows the predicted curvature of the DRE. Note that the curvature of the DRE is less than that of the synthetic AT curves; the DNA is curved by roughly 60° over about 100–120 bp.

Gel Mobility—Although the DNA fragments were predicted to be either curved or noncurved, it was necessary to demonstrate this experimentally. One commonly used method for assessing DNA curvature is anomalous mobility on polyacrylamide gels (38). Fig. 3 shows the relative mobility of the five synthetic DNA fragments and the DRE. The apparent sizes of the fragments under these conditions were estimated from their mobilities with respect to molecular weight markers. The " R_L values," the ratios of the apparent sizes to the actual sizes of the fragments, were as follows: GC noncurve, 1.0; GC curve, 1.3; AT curve, 2.8; AT noncurve, 1.0; AT planar curve, 2.1, DRE, 1.2. The curvatures measured experimentally under these conditions were consistent with the computer predictions.

Binding of H-NS to Curved and Noncurved DNA Fragments by Bandshift

The relative affinity of H-NS for curved and noncurved DNA fragments was initially assessed by bandshift assays. Plasmids containing the curved and noncurved DNA fragments (pAF1–3; pAF6; pTP4–5) were digested with *Hae*III, incubated with different amounts of H-NS, and electrophoresed in agarose gels. Fig. 4 shows that, in general, the larger the DNA fragment, the lower the H-NS concentration required to initiate a bandshift. This is consistent with H-NS binding nonspecifically to generic DNA. However, the fragment containing the AT planar curve was "shifted" at an approximately 5-fold lower H-NS concentration than the other fragments of similar size, demonstrating a small binding preference for this curve. In contrast, no significant preference could be detected for the nonplanar AT curve (Fig. 4). As the AT curve and AT planar curve differ in the planarity of the curve, this observation demonstrates a role for the specific architecture of the curve in determining binding preference. Importantly, in the same assay, H-NS did not show a detectable binding preference for any of the other curved or noncurved fragments, including the DRE (data not shown).

An alternative assay that has been used previously to show that H-NS has a binding preference for curved compared with noncurved DNA fragments is a competition bandshift. DNA

TABLE II
Plasmid constructions

Plasmid	Vector	Insert/construction	Ref.
pBluescript			Stratagene
pTP4	pBluescript II KS (+)	120 bp, AT curve	13
pTP5	pBluescript II KS (+)	105 bp, AT noncurve	13
pAF1	pBluescript I SK (-)	214 bp, GC noncurve	This study
pAF2	pBluescript I SK (-)	193 bp, GC curve	This study
pAF3	pBluescript I SK ()	105 bp, AT planar curve	This study
pAF6	pBluescript II SK (-)	200 bp, DRE (+99 to +299)	This study
pSB71	<i>luxAB</i> promoter cloning vector		45
pSJ4	pSB71	<i>proU</i> promoter (-217 to +100)	46
pBJ1	pSJ4	<i>NcoI</i> and <i>BglI</i> site introduced (see Fig. 1)	This study
pBJ2	pBJ1	<i>trp-lacZ</i> fusion	This study
pBJ4	pBJ1	CCGAT	This study
pBJ5	pBJ1	CCGATGAAAG	This study
pBJ6	pBJ1	CCGATGAAAGCGGCG	This study
pAV399	<i>proU</i> promoter fused to <i>lacZ</i> (no DRE)		13
pAV260	<i>proU</i> promoter fused to <i>lacZ</i> (with DRE)		13
pAV280	pAV260 with <i>proU</i> promoter deleted		43
pAF450	pAV399	51-bp polylinker introduced ^a	This study
pAF451	pAF450	214 bp, GC noncurve	This study
pAF452	pAF450	193 bp, GC curve	This study
pAF453	pAF450	105 bp, AT planar curve	This study
pAF454	pAF450	120 bp, AT curve	This study
pAF455	pAF450	105 bp, AT noncurve	This study
pAF456	pAF450	DRE (+99 to +299)	This study

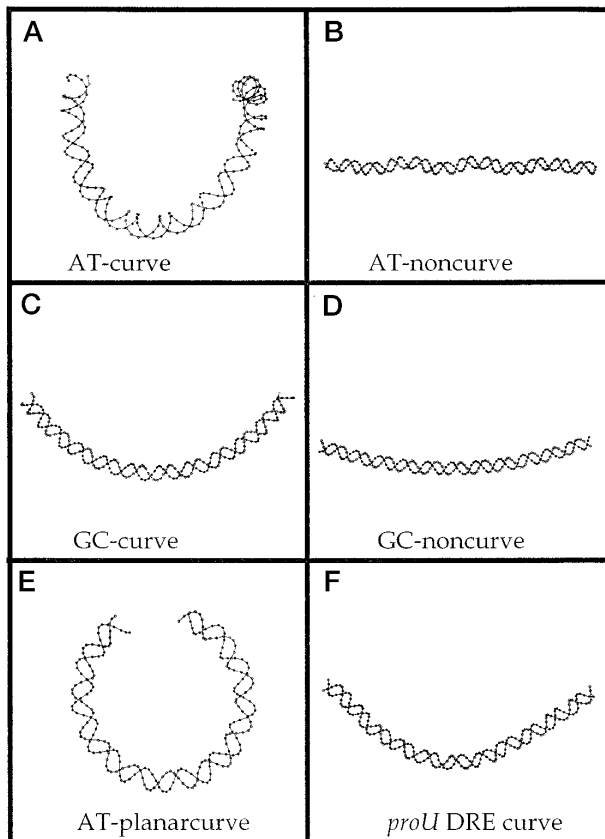
^a See "Experimental Procedures."

FIG. 2. Predicted DNA paths of 120-bp synthetic DNA fragments used in this study. The DNA sequences of the oligonucleotides used to generate each fragment are as in Table I. Panel A, AT curve; panel B, AT noncurve; panel C, GC curve; panel D, GC noncurve; panel E, AT planar curve; panel F, the endogenous curve downstream of the chromosomal *proU* gene of *S. typhimurium* (the DRE; bp 62–182). The predicted DNA paths were calculated using the CURVATURE program (37).

fragments were isolated and end-labeled with [³²P]dATP. In each assay, one DNA fragment was radiolabeled and incubated with sufficient H-NS to form a discrete bandshifted protein-

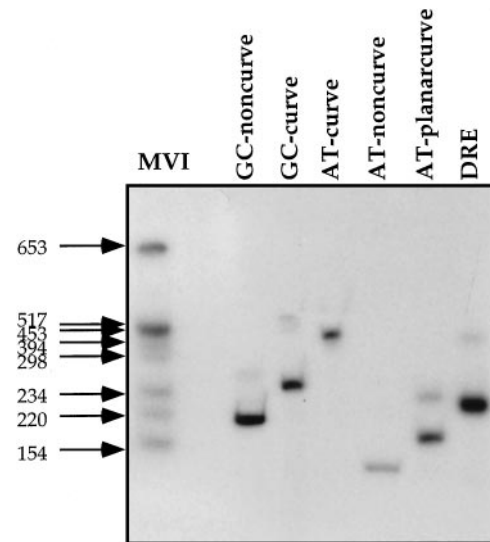


FIG. 3. Electrophoretic mobility of six curved and noncurved DNA fragments. DNA fragments isolated from plasmids pAF1 (GC noncurve); pAF2 (GC curve); pAF3 (AT planar curve); pTP4 (AT curve); pTP5 (AT noncurve); or pAF6 (DRE) were loaded onto a 12% polyacrylamide gel and electrophoresed at 4 °C in TBE buffer for 4 h at 8 V/cm. The molecular weight marker is MVI (Boehringer Mannheim). DNA was visualized by ethidium bromide staining.

DNA complex. Excess unlabeled competitor DNA fragment was then added to 1, 10, or 100 × the mass of labeled fragment. Addition of competitor DNA reduced the amount of "bandshifted" complex that could be quantitated by densitometry. An example of such an experiment is shown in Fig. 5. When the AT curve fragment was labeled (lanes a–h), addition of 10-fold excess of the AT curve competitor fragment abolished the bandshifted complex (lane d). In contrast, 10-fold excess of the AT noncurve competitor fragment (lane g) had little effect, and 100-fold excess was required to prevent complex formation (lane h). Thus, consistent with previous data (12, 13, 18) H-NS has a greater affinity for the AT curve fragment than for the AT noncurve fragment, although the difference in affinity is less than an order of magnitude.

A similar experiment (Fig. 5) shows that H-NS has a higher

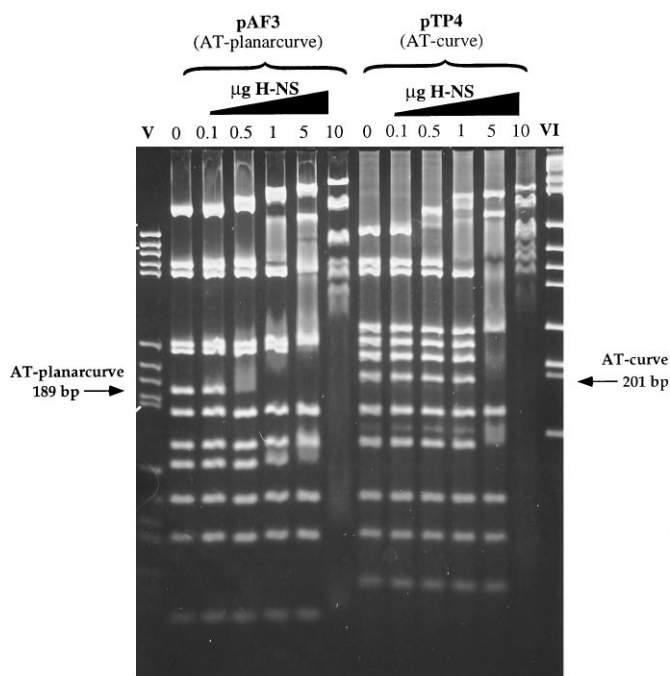


FIG. 4. H-NS shows binding preference for the AT planar curve. Increasing amounts of H-NS were incubated with DNA of plasmid pAF3 or pTP4 digested with *Hae*III. The *Hae*III fragments containing curved inserts, the AT planar curve (189 bp), and the AT curve (201 bp), are indicated by arrows. Lanes V and VI are molecular weight markers (Boehringer Mannheim). DNA was visualized by ethidium bromide staining.

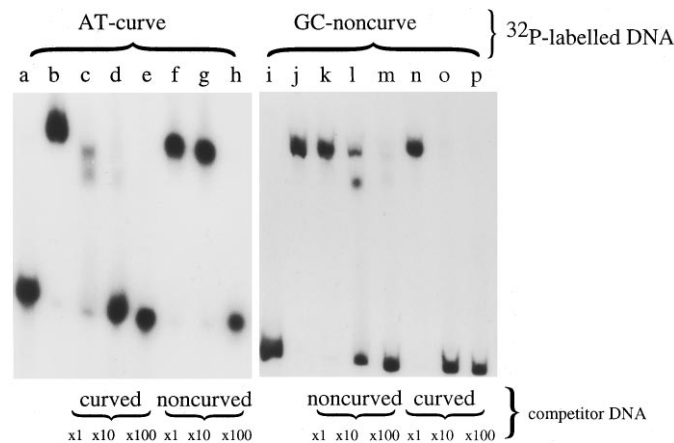


FIG. 5. Relative binding affinity of H-NS for different curved and noncurved DNA fragments by competition bandshift. The relative affinity of H-NS for the AT curve, the AT noncurve, the GC curve, and the GC noncurve were compared in a competition bandshift assay. Lanes a–h, the AT curve was radiolabeled. Lane a, DNA alone; lane b, DNA with H-NS showing bandshifted complex; lanes c–e, DNA with H-NS (as for lane b) with 1, 10, and 100 × competitor AT curve added; lanes f–h, DNA with H-NS (as for lane b) with 1, 10, and 100 × competitor AT noncurve added. Lanes i–p, the GC noncurve was radiolabeled. Lane i, DNA alone; lane j, DNA with H-NS showing bandshifted complex; lanes k–m, DNA with H-NS (as for lane j) with 1, 10, and 100 × competitor GC noncurve added; lanes n–p, DNA with H-NS (as for lane j) with 1, 10, and 100 × GC curve competitor added.

affinity for the GC curve than the GC noncurve; this difference in affinity is similar to the difference between the AT curve and AT noncurve. Thus, the preferential affinity for curved DNA is not restricted to A tract curves; and curvature, rather than base composition, determines H-NS binding preference. As H-NS binds the AT planar curve better than the nonplanar AT curve, the specific architecture of the curve is also important. However, in no case was the affinity for any sequence, includ-

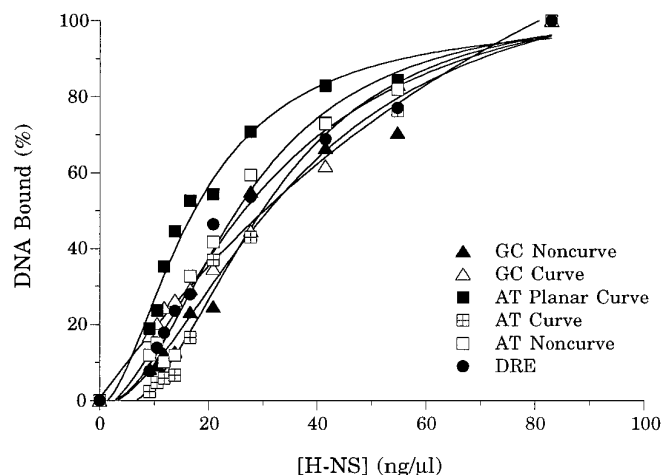


FIG. 6. Filter retention assays. The concentration dependence of the interaction of H-NS with different radiolabeled DNA fragments was determined by filter retention. The maximum fraction of DNA bound varied experimentally from 90 to 100%. The data are expressed, for comparative purposes, as the percent of the maximal fraction bound. The values are the average of three independent experiments.

ing the DRE, greater than a few-fold higher than for noncurved or generic DNA.

H-NS-DNA Interactions by Filter Retention

To obtain a more quantitative comparison of the apparent affinity of H-NS for the different curved and noncurved DNA fragments, we used a nitrocellulose filter retention assay. In this assay no significant binding preference for any of the DNA ligands tested was detected; all the DNA fragments were retained by H-NS to a similar extent (nearly 100%) and with a similar concentration dependence (Fig. 6). To confirm that the assay was measuring concentration dependence and not the stoichiometry of the H-NS-DNA interaction, we repeated the binding studies with different amounts of DNA ligand (10 and 50 ng) and obtained indistinguishable binding curves (data not shown). The apparent K_d values, assuming that the H-NS preparation was 100% active and that H-NS interacts with DNA as a monomer, were calculated by curve-fitting analysis. The apparent K_d values for the interaction of H-NS with all of the sequences were similar, although the AT planar curve bound slightly better ($K_d = 1.0 \mu\text{M}$) than the other fragments ($K_d = 1.6\text{--}2.3 \mu\text{M}$).

Thus, no significant difference in affinity of H-NS for any sequence, including the DRE, could be detected by filter retention. This is in apparent contrast to bandshift studies that showed slightly enhanced affinity for curved sequences. This difference is likely to be due to differences in the rates of association and dissociation of the protein-DNA complexes during electrophoresis which may contribute to the apparent specificity of the interaction under bandshift conditions. However, measurement of differences in the on and off rates of the H-NS-DNA complexes with curved and noncurved DNA ligands using the filter retention assay was precluded by the rapid interaction kinetics of H-NS with DNA: the complex forms and dissociates within 10 s (not shown).

The Distance between the *proU* Promoter and the Downstream Curve Is Unimportant *In Vivo*

To ascertain whether the relative efficiency with which the curved and noncurved sequences bind H-NS *in vitro* reflects their activity *in vivo*, the ability of these sequences to replace the function of the DRE *in vivo* was assessed. The DRE is located approximately 200 bp downstream of the *proU* pro-

TABLE III
Effect of insertions between the promoter and downstream curve on *proU* promoter activity

Plasmids contain the *proU* promoter upstream of the *luxAB* reporter genes. Luciferase activity in the *S. typhimurium hns*⁺ strain CH1833 was measured at low and high osmolarity as a measure of *proU* promoter activity.

Plasmid	Insertion bp	Luciferase activity	
		Low	High
pBJ1	0	0.62	256.4
pBJ4	5	3.68	324.8
pBJ5	10	0.48	231.7
pBJ6	15	2.01	232.0
pBJ2	210	2.56	50.0

motor and is required for H-NS-mediated repression of transcription. Before replacing the DRE with heterologous sequences, it was necessary to ensure that the precise distance between the promoter and downstream curve is not important. Thus, defined oligonucleotides were introduced between the *proU* promoter and the *lux* reporter gene in plasmid pBJ1, increasing the distance between the *proU* promoter and the downstream curve by 5, 10, 15, or 210 bp (Fig. 1). *proU* promoter activity of each of these plasmids was monitored by measuring *lux* reporter gene activity in *S. typhimurium hns*⁺ strain CH1833 (Table III). Increasing the distance between the *proU* promoter and the downstream curve had no major effect on osmoregulation of transcription, although the 210-bp fragment did reduce the absolute magnitude of expression somewhat. As the insertion of a nonintegral number of turns of the DNA helix (5 or 15 bp) will change the "face of the helix" of the curve relative to the *proU* promoter, it appears that the orientation of the curve with respect to the promoter is relatively unimportant. Thus, the distance between the promoter and the DRE, and their relative orientations with respect to the face of the helix, can be varied with little effect on expression or regulation. This is consistent with other reports (26). Importantly, this result ensures that interpretation of the following *in vivo* experiments is not influenced by the precise position at which the curves were inserted.

Ability of Curved and Noncurved DNA Fragments to Replace DRE Function *in Vivo*

Plasmid pAF450 contains a segment of the *proU* promoter extending from -219 to +100 fused to the *lacZ* reporter gene. This plasmid lacks the DRE, and hence, the *proU* promoter is derepressed and exhibits minimal osmoregulation. Curved and noncurved DNA fragments were inserted into the polylinker between the *proU* promoter and the *lacZ* reporter gene in this plasmid (see "Experimental Procedures" and Table II). The resultant plasmids were electroporated into wild-type *S. typhimurium* (LT2) and β -galactosidase expression measured at low osmolarity and after osmotic upshock (0.3 M NaCl). The ratio of expression at high to low osmolarity, the induction ratio, indicates the degree of osmoregulation.

Plasmid pAV260 which contains the *proU* promoter region from -207 to +736, and therefore includes the DRE, served as a positive control. Promoter activity was tightly osmoregulated (induction ratio = 63.0) (Table IV). The *proU* promoter in plasmid pAF450, from which the DRE was deleted, was derepressed at low osmolarity such that the osmotic induction ratio was severely reduced (induction ratio = 7.3). These results with the control plasmid were as expected (13). It should be noted that, as reported previously, residual osmotic regulation was observed when the DRE was deleted showing that sequences other than the DRE play some role in regulation (13, 26, 28). Re-insertion of the DRE between the promoter and *lacZ*

restored normal osmoregulation (pAF456; induction ratio of 71.0). Although the DRE is translated in its natural location within the first structural gene of the *proU* operon, in this plasmid the DRE is not translated. As normal osmoregulation was observed, this demonstrates that the influence of the DRE on *proU* transcription is independent of translation. In contrast to the DRE, none of the other curved or noncurved fragments, including the AT planar curve, restored osmoregulation when inserted at the same site in pAF450.

The plasmids were also introduced into the congenic *hns* strain CH1838. As expected for the positive control plasmid pAV260, expression at low osmolarity was severely derepressed such that the induction ratio was reduced from 63.0 to 2.0 (Table IV). A similar derepression at low osmolarity, reducing the induction ratio (71.0 to 1.3), was seen for plasmid pAF456 into which the DRE had been reinserted. Thus, as reported previously, repression of the *proU* promoter at low osmolarity requires both H-NS and the DRE.

Importantly, for the plasmid with the AT planar curve inserted (pAF453), *proU* expression was derepressed in the *hns* strain compared with the *hns*⁺ strain. Thus, it appears that H-NS interacts with this curve *in vivo*. However, in the *hns*⁺ strain the AT planar curve did not lead to full repression, in contrast to the DRE. Thus, the binding of H-NS to the AT planar curve only partially represses transcription, whereas H-NS binding to the DRE results in full repression.

It is important to note that, in the absence of H-NS, the nature of the sequence inserted downstream of the *proU* promoter influenced the basal level of expression. Most notably, the DRE and AT planar curve led to maximum derepression at both low and high osmolarity (19,280 and 18,974 units, respectively, at low osmolarity). In contrast, the other sequences achieve a degree of repression even in the absence of H-NS. This is most obvious for the GC curve and AT curve (pAF452 and pAF454, respectively) where expression at low osmolarity in the presence of H-NS was 1226 and 2466 units, respectively, which only increased to 2114 and 2121 units in the absence of H-NS. This implies that the overall configuration of the downstream region is important for optimal transcription, irrespective of the presence or absence of H-NS.

DISCUSSION

To understand the role of H-NS in the bacterial cell, and specifically the mechanism by which it influences transcription, it is necessary to understand how this protein interacts with DNA. It has previously been reported that, although H-NS binds nonspecifically to any DNA molecule, it has enhanced binding to intrinsically curved DNA. Furthermore, at least some of the *in vivo* sites of action of H-NS are curved. This led to the hypothesis that the interaction of H-NS with curved DNA is important for its mode of action. In this study we have tested this hypothesis, asking two questions: whether DNA curvature *per se* determines the specificity of action of H-NS, and whether the binding of H-NS to curved DNA is sufficient to account for the effects of H-NS on gene expression.

H-NS has previously been shown, by bandshift studies, to exhibit a binding preference for intrinsically curved DNA elements generated by phased A tracts (11-13). We have shown here that H-NS has a similar binding preference for non-A tract curves (GC curves). Thus DNA curvature, rather than the specific presence of A tracts, appears to be responsible for this H-NS binding preference. In addition, H-NS bound more strongly to a planar curve than to a nonplanar curve of similar base composition, showing that the specific architecture of the curve also influences H-NS binding. However, in these bandshift studies the maximum preference for any curved sequence tested, including the DRE, was only a few-fold greater than for

TABLE IV
Effects of various curved and noncurved DNA on *proU* promoter function

β -Galactosidase expression from plasmids in *S. typhimurium* LT2 or its *hns* derivative CH1838 was assayed at low and high osmolarity. The induction ratios indicate the fold increase in expression at high osmolarity compared with expression at low osmolarity.

Plasmid	β -Galactosidase activity				Induction ratios	
	LT2		CH1838		Wild type (LT2)	<i>hns</i> mutant (CH1838)
	Low	High	Low	High		
pAV260 positive control	311	19,466	11,295	23,105	63.0	2.0
pAF450 no insert	1,761	12,978	8,662	16,758	7.3	1.9
pAF456 DRE curve	158	11,209	19,280	25,027	71.0	1.3
pAF453 AT planar curve	3,922	10,227	18,974	17,500	2.6	0.9
pAF451 GC noncurve	1,243	10,327	6,975	12,093	8.3	1.7
pAF452 GC curve	1,226	7,230	2,114	6,096	5.9	2.9
pAF454 AT curve	2,466	8,114	2,121	6,518	3.3	3.1
pAF455 AT noncurve	3,941	7,918	8,569	9,179	2.0	1.1

generic DNA. This is consistent with previous reports that H-NS shows a binding preference for curved DNA; these other studies also used similar bandshift assays, and all demonstrated less than a 10-fold preference for any curved DNA fragment compared with generic DNA (11–14, 18).

In apparent contrast to the bandshift experiments, filter retention experiments failed to reveal any major binding preference of H-NS for curved DNA or for the DRE. Although the AT planar curve did bind with slightly higher K_d than the other fragments tested, this was only by about 2-fold. The difference between bandshift and filter-retention studies probably reflects differences in on/off rates for the different sequences which during electrophoresis could influence apparent binding affinities in bandshift experiments. However, the on/off rates were too fast to permit measurement of any differences in these parameters. Despite the apparent difference in conclusions reached using the two methodologies it is more important to emphasize the similarities: in neither type of assay was more than about a 5-fold binding preference for any sequence observed. Furthermore, the binding preference for the DRE was slight and less than for the AT planar curve. Thus, it is clear that the binding preference for curved DNA, or the native DRE, cannot account for the specificity of H-NS action.

The filter retention experiments allowed the K_d of H-NS binding to DNA ligands to be estimated as 1–2 μM , assuming that the H-NS preparation was 100% active and that H-NS interacts with DNA as a monomer. As H-NS is able to form oligomers (15),² the actual K_d value may be somewhat lower. Thus, the affinity of H-NS for DNA is relatively poor in comparison with classical sequence-specific regulatory proteins, although better than nonspecific binding of proteins to DNA. For example, the integration host factor interacts with its specific sites with high affinity ($K_d \approx 50 \text{ nM}$) and with generic DNA with a K_d of about 20 μM (39). Instead, H-NS interacts with DNA with similar affinity to HU, the other major chromatin-associated protein in *E. coli*, which has a K_d for generic DNA molecules of about 1 μM (40). The low affinity of the H-NS-DNA interaction cannot be reconciled with a classical repressor-type mechanism for modulating gene expression.

At the *proU* promoters of *E. coli* and *S. typhimurium*, H-NS represses transcription by binding to the DRE, located some 100–200 bp downstream of the transcription start site (13, 25, 26). To determine whether H-NS binding *per se* is sufficient to maintain repression of the *proU* promoter, defined sequences were cloned between the *proU* promoter and a downstream reporter gene, replacing the DRE. As a control we showed that the precise distance between the *proU* promoter and the DRE, and their relative orientations on the face of the helix, had little

effect on H-NS-mediated repression of transcription. This is consistent with previously published data (26, 28). Insertion of the DRE between the *proU* promoter and *lacZ* reporter gene restored H-NS-mediated repression at low osmolarity, as expected. However, none of the other curved or noncurved sequences tested could replace the DRE (although it should be noted that we have previously shown that a heterologous intrinsic curve from the *luxAB* genes can replace the DRE; 13). Even the AT planar curve, to which H-NS binds with higher affinity than it does to the DRE, could not functionally replace the DRE. Previous studies have indicated that H-NS binds to the AT planar curve *in vivo* (17), and in this study the effect of the AT planar curve is altered in an *hns* mutant implying that H-NS binds to this curve *in vivo*. Thus, the binding of H-NS to a downstream curved sequence *per se* is insufficient to repress *proU* transcription. This argues strongly against classical repressor-type models in which H-NS directly occludes RNA polymerase binding at the *proU* promoter. These findings suggest that the DRE is not simply a specific binding site for H-NS but, instead, acts as an effector site for H-NS action. One possible mechanism by which the DRE might act as an effector is by undergoing specific topological changes in response to the interaction of H-NS. This is consistent with the findings reported here that, even in the absence of H-NS, the nature of the downstream sequence influences promoter activity, with published data showing that the *proU* promoter is sensitive to topological changes (6, 13, 41) and with observations that H-NS influences DNA topology (5–9). The simplest model consistent with available data is that, in the absence of H-NS, the DRE allows the promoter to adopt an architecture leading to maximum promoter activity. When H-NS binds to the DRE it alters the architecture of the promoter region and, hence, represses transcription. These architectural changes could involve DNA flexibility (the *proU* promoter is activated by increased DNA flexibility; 41) and/or DNA looping. There is accumulating evidence that H-NS distorts DNA, although the nature of this distortion is unclear: H-NS can constrain DNA supercoils *in vitro* (5), it can act at a distance *in vivo* (13, 17, 28), and it generates DNase I-hypersensitive sites on binding (5, 13, 16). Although *proU* is simpler than other H-NS-dependent promoters, in that it does not appear to require additional *trans*-acting factors, there is no *a priori* reason why similar mechanisms should not operate at many other H-NS-dependent promoters; positive regulators may alter local promoter architecture to overcome H-NS repression (42).

Most H-NS-dependent genes are regulated in response to environmental signals. DNA curvature changes significantly in response to altered environmental conditions (19),² and it is tempting to postulate that, at simple promoters such as *proU*, the structure of the DRE itself may act as an “environmental sensor”; environmentally induced changes in DNA configura-

²D. W. Ussery, C. F. Higgins, and A. Bolshoy, submitted for publication.

tion influence the action of H-NS, leading to an alteration in promoter configuration and, hence, transcription. Furthermore, as different DNA sequences respond to different environmental cues (19),³ it is possible to envisage a mechanism by which H-NS can regulate specific genes in response to different environmental signals. The possibility that environmental signals may directly affect promoter architecture and hence transcription, through influencing the interaction of architectural proteins with DNA, may be an important concept in understanding the environmental regulation of gene expression in bacteria.

Acknowledgments—We thank Francisco Mojica, Jean Sonnenfeld, Robert Stephen, and Stephen Gunn for helpful discussions. Tom Owen-Hughes assisted with some of the plasmid constructions and Clare Smyth and Julie Sidebotham with H-NS purification.

REFERENCES

- Higgins, C. F., Hinton, J. C. D., Hulton, C. S. J., Owen-Hughes, T. A., Pavitt, G. D., and Seirafi, A. (1990) *Mol. Microbiol.* **4**, 2007–2012
- Ussery, D. W., Hinton, J. C. D., Jordi, B. J. A. M., Granum, P. E., Seirafi, A., Stephen, R. J., Tupper, A. E., Berridge, G., Sidebotham, J. M., and Higgins, C. F. (1994) *Biochimie (Paris)* **76**, 968–980
- Spassky, A., Rimsky, S., Garreau, H., and Buc, H. (1984) *Nucleic Acids Res.* **12**, 5321–5340
- Spurio, R., Dürrenberger, M., Falconi, M., La Teana, A., Pon, C. L., and Gualerzi, C. O. (1992) *Mol. & Gen. Genet.* **231**, 201–211
- Tupper, A. E., Owen-Hughes, T. A., Ussery, D. W., Santos, D. S., Ferguson, D. J., Sidebotham, J. M., Hinton, J. C. D., and Higgins, C. F. (1994) *EMBO J.* **13**, 258–268
- Higgins, C. F., Dorman, C. J., Stirling, D. A., Waddell, L., Booth, I. R., May, G., and Bremer, E. (1988) *Cell* **52**, 569–584
- Hulton, C. S. J., Seirafi, A., Hinton, J. C. D., Sidebotham, J. M., Waddell, L., Pavitt, G. D., Owen-Hughes, T. A., Spassky, A., Buc, H., and Higgins, C. F. (1990) *Cell* **63**, 631–642
- Hinton, J. C. D., Santos, D. S., Seirafi, A., Hulton, C. S. J., Pavitt, G. D., and Higgins, C. F. (1992) *Mol. Microbiol.* **6**, 2327–2337
- Mojica, F. J. M., and Higgins, C. F. (1997) *J. Bacteriol.*, in press
- Friedrich, K., Gualerzi, C. O., Lammi, M., Losso, M. A., and Pon, C. L. (1988) *FEBS Lett.* **229**, 197–202
- Bracco, L., Kotlarz, D., Kolb, A., Diekmann, S., and Buc, H. (1989) *EMBO J.* **8**, 4289–4296
- Yamada, H., Muramatsu, S., and Mizuno, T. (1990) *J. Biochem. (Tokyo)* **108**, 420–425
- Owen-Hughes, T. A., Pavitt, G. D., Santos, D. S., Sidebotham, J. M., Hulton, C. S. J., Hinton, J. C. D., and Higgins, C. F. (1992) *Cell* **71**, 255–265
- Tippner, D., and Wagner, R. (1995) *J. Biol. Chem.* **270**, 22243–22247
- Falconi, M., Higgins, N., Spurio, R., Pon, C., and Gualerzi, C. O. (1993) *Mol. Microbiol.* **10**, 273–282
- Tippner, D., Afflerbach, H., Bradaczek, C., and Wagner, R. (1994) *Mol. Microbiol.* **11**, 589–604
- Zuber, F., Kotlarz, D., Rimsky, S., and Buc, H. (1994) *Mol. Microbiol.* **12**, 231–240
- Ueguchi, C., Suzuki, T., Yoshida, T., Tanaka, K.-I., and Mizuno, T. (1996) *J. Mol. Biol.* **263**, 149–162
- Pérez-Martín, J., Rojo, F., and De Lorenzo, V. (1994) *Microbiol. Rev.* **58**, 268–290
- Cairney, J., Booth, I. R., and Higgins, C. F. (1985) *J. Bacteriol.* **164**, 1224–1232
- Dunlap, V. J., and Csonka, L. N. (1985) *J. Bacteriol.* **163**, 296–304
- Gowrishankar, J. (1985) *J. Bacteriol.* **164**, 434–445
- May, G., Faatz, E., Villarejo, M., and Bremer, E. (1986) *Mol. & Gen. Genet.* **205**, 225–233
- May, G., Dersch, P., Haardt, M., Middendorf, A., and Bremer, E. (1990) *Mol. & Gen. Genet.* **224**, 81–90
- Lucht, J. M., Dersch, P., Kempf, B., and Bremer, E. (1994) *J. Biol. Chem.* **269**, 6578–6586
- Fletcher, S. A., and Csonka, L. N. (1995) *J. Bacteriol.* **177**, 4508–4513
- Dattananda, C. S., Rajkumari, K., and Gowrishankar, J. (1991) *J. Bacteriol.* **173**, 7481–7490
- Overdier, D. G., and Csonka, L. N. (1992) *Proc. Natl. Acad. Sci. U. S. A.* **89**, 3140–3144
- Bertani, G. (1951) *J. Bacteriol.* **62**, 293–300
- Stirling, D. A., Hulton, C. S. J., Waddell, L., Park, S. F., Stewart, G. S., Booth, I. R., and Higgins, C. F. (1989) *Mol. Microbiol.* **3**, 1025–1038
- Simons, R. W., Housman, F., and Kleckner, N. (1987) *Gene (Amst.)* **53**, 85–96
- Sambrook, J., Fritsch, E. F., and Maniatis, T. (1989) *Molecular Cloning: A Laboratory Manual*, 2nd Ed., Cold Spring Harbor Laboratory, Cold Spring Harbor, NY
- McNamara, P. T., Bolshoy, A., Trifonov, E. N., and Harrington, R. E. (1990) *J. Biomol. Struct. & Dyn.* **8**, 529–538
- McNamara, P. T., and Harrington, R. E. (1991) *J. Biol. Chem.* **266**, 12548–12554
- Bolshoy, A., McNamara, P., Harrington, R. E., and Trifonov, E. N. (1991) *Proc. Natl. Acad. Sci. U. S. A.* **88**, 2312–2316
- Ulanovsky, L., Bodner, M., Trifonov, E. N., and Choder, M. (1986) *Proc. Natl. Acad. Sci. U. S. A.* **83**, 862–866
- Shpigelman, E. S., Trifonov, E. N., and Bolshoy, A. (1993) *Comput. Appl. Biosci.* **9**, 435–440
- Crothers, D. M., Haran, T. E., and Nadeau, J. G. (1990) *J. Biol. Chem.* **265**, 7093–7096
- Yang, S.-W., and Nash, H. A. (1995) *EMBO J.* **14**, 6292–6300
- Bonnefoy, E., Takahashi, M., Rouviere-Yaniv, J. R. (1994) *J. Mol. Biol.* **242**, 116–129
- Jordi, B. J. A. M., Owen-Hughes, T. A., Hulton, C. S. J., and Higgins, C. F. (1995) *EMBO J.* **14**, 5690–5700
- Jordi, B. J. A. M., Dagberg, B., de Haan, L. A. M., Hamers, A. M., van der Zeijst, B. A. M., Gaastra, W., and Uhlin, B. E. (1992) *EMBO J.* **11**, 2627–2632
- Pavitt, G. D., and Higgins, C. F. (1993) *Mol. Microbiol.* **10**, 685–696
- Koo, H. S., Wu, H. M., and Crothers, D. M. (1986) *Nature* **320**, 501–506
- Park, S. F., Stirling, D. A., Hulton, C. S. J., Booth, I. R., Higgins, C. F., and Stewart, G. S. A. B. (1989) *Mol. Microbiol.* **3**, 1011–1023
- Hulton, C. S. J. (1993) *Molecular Genetic Analysis of the Supercoiling Regulated proU Promoter of Salmonella typhimurium*. Ph.D. thesis, St. Cross College, University of Oxford